Journal of Physiology (1993), **468**, *pp.* 669–691
With 12 *figures*
Printed in Great Britain

MECHANISMS OF OSCILLATORY ACTIVITY IN GUINEA-PIG NUCLEUS RETICULARIS THALAMI *IN VITRO*: A MAMMALIAN PACEMAKER

BY THIERRY BAL AND DAVID A. McCORMICK

From the Section of Neurobiology, Sterling Hall of Medicine C303, Yale University Medical School, 333 Cedar Street, New Haven, CT 06510, USA

(*Received 3 September 1992*)

SUMMARY

1. The ionic mechanisms of rhythmic burst firing and single spike, tonic discharge were investigated with extracellular and intracellular recordings of single neurones in the guinea-pig nucleus reticularis thalami (NRT) maintained as a slice *in vitro*.

2. Activation of cortical/thalamic afferents to NRT neurones resulted in a short latency burst of action potentials which could be followed by a rhythmic sequence of oscillatory burst firing. Intracellularly, this oscillatory activity was associated with an alternating sequence of low threshold Ca^{2+} spikes separated by after-hyperpolarizing potentials. Intracellular injection of short duration hyperpolarizing current pulses resulted in a similar sequence of oscillatory burst firing, suggesting that this activity is an intrinsic property of NRT cells. The frequency of rhythmic burst firing was highly voltage and temperature dependent and was between 7–12 Hz at −65 to −60 mV at 38 °C. In addition, at depolarized membrane potentials, oscillatory burst firing was typically followed by a prolonged tail of single spike activity.

3. Application of the Na^+ channel poison tetrodotoxin blocked the generation of fast action potentials, but left intact the rhythmic sequence of low threshold Ca^{2+} spikes separated by after-hyperpolarizing potentials (AHPs). The reversal potential of the AHPs was −94 mV, suggesting that it was mediated by an increase in K^+ conductance. Extracellular application of tetraethylammonium or apamin, or intracellular injection of Cs^+ or the Ca^{2+} chelating agent EGTA, blocked the Ca^{2+} spike AHP, indicating that it is mediated by a Ca^{2+}-activated K^+ current.

4. Block of the AHP resulted in the marked enhancement of a slow after-depolarizing potential (ADP). The slow ADP occurred only following the generation of low threshold Ca^{2+} spikes. Replacement of extracellular Ca^{2+} with Mg^{2+} or Sr^{2+} resulted in an abolition of the slow ADP. In addition, the increase in $[Mg^{2+}]_o$ resulted in an abolition of the low threshold Ca^{2+} spike. In contrast, replacement of extracellular Ca^{2+} with Ba^{2+} did not abolish the slow ADP. These results indicate that the ADP can be activated by either Ca^{2+} or Ba^{2+}, but not by Mg^{2+} or Sr^{2+}.

5. Replacement of extracellular Na^+ with choline$^+$ did not abolish the slow ADP, while replacement with *N*-methyl-D-glucamine$^+$ did, indicating that the slow ADP

can be supported by choline$^+$, but not by *N*-methyl-D-glucamine$^+$. Neither chemical affected the low threshold Ca^{2+} spike. These results are consistent with the slow ADP being mediated by a Ca^{2+}-activated non-selective cation (CAN) current.

6. Application of maximal doses of noradrenaline resulted in a shift to highly regular single spike activity at 30–40 Hz at 38 °C, while maximal doses of serotonin or the glutamate metabotropic receptor agonist 1S,3R-1-aminocyclopentane-1,3-dicarboxylic acid (ACPD) resulted in peak firing frequencies of 55–65 Hz at 38 °C. Intracellularly, this shift to tonic firing was associated with depolarization of the membrane and a decrease in apparent input conductance.

7. Application of tetrodotoxin during tonic, single spike activity induced by serotonin resulted in abolition of Na^+ spikes and a hyperpolarization of the membrane potential of 3–6 mV, indicating that the persistent Na^+ current contributes substantially to the determination of the frequency of action potential discharge during this mode of activity.

8. We suggest that nucleus reticularis neurones possess three distinct modes of oscillatory activity: (1) slow (0·5–7 Hz) rhythmic burst firing at hyperpolarized membrane potentials resulting from the interaction of the low threshold Ca^{2+} current and a Ca^{2+}-activated K^+ current; (2) rhythmic burst firing in the frequency range of spindle waves (7–12 Hz) followed by a tonic 'tail' of single spike activity resulting from the interaction of the low threshold Ca^{2+} current and an apamin-sensitive, Ca^{2+}-activated K^+ current and the activation of a Ca^{2+}-activated non-selective cation (CAN) current; and (3) tonic, 30–60 Hz single spike activity which appears during maximal block of resting, leak K^+ current by 5-HT, noradrenaline or ACPD and which results from an new equilibrium between the currents involved in action potential generation and the persistent Na^+ current.

INTRODUCTION

The nucleus reticularis thalami (NRT) forms a shell that surrounds much of the dorsal and lateral extent of the dorsal thalamus (Jones, 1985). It is composed of GABAergic neurones and projects heavily to nearly every nucleus of the thalamus, and innervates relay cells (Houser, Vaughn, Barber & Roberts, 1980; Steriade, Parent & Hada, 1984; Yen, Conley, Hendry & Jones, 1985). Thalamocortical and corticothalamic fibres densely innervate the NRT with axon collaterals as the parent axons transverse this structure (Ohara & Lieberman, 1981, 1985; Harris, 1987). In addition, neurones in the NRT are also innervated by noradrenergic fibres from the locus coeruleus (see Asanuma, 1992), serotoninergic fibres from the raphe (Wilson & Hendrickson, 1988; Lavoie & Parent, 1991), cholinergic fibres from the brainstem and basal forebrain cholinergic groups (Hallanger, Levey, Lee, Rye & Wainer, 1987; Levey, Hallanger & Wainer, 1987; Steriade, Parent, Paré & Smith, 1987 *b*; Asanuma, 1989), and GABAergic fibres from the basal forebrain, substantia nigra reticulata, and the external field of the globus pallidus (Asanuma, 1989; Asanuma & Porter, 1990; Paré, Hazrati, Parent & Steriade, 1990; Hazrati & Parent, 1991). Local axon collaterals within the NRT, as well as dendrodendritic synapses in the cat and primate, serve as an additional source of GABAergic innervation of these neurones (see Deschênes, Madariaga-Domich & Steriade, 1985;

Yen *et al.* 1985; Shosaku, Kayama, Sumitomo, Sugitani & Iwama, 1989).

In vivo, NRT cells display two distinct modes of action potential generation: rhythmic burst firing during periods of synchronized electroencephalogram activity such as during slow wave sleep (Mulle, Madariaga & Deschênes, 1986; Steriade, Domich & Oakson, 1986) and absence seizures (Buzsáki, Bickford, Ponomareff, Thal, Mandel & Gage, 1988) and single spike firing during wakefulness or rapid-eye-movement sleep (Mukhametov, Rizolatti & Seitun, 1970*a*; Mukhametov, Rizzolatti & Tradardi, 1970*b*; Steriade *et al.* 1986). Spontaneous rhythmic burst firing during slow-wave sleep in the NRT often occurs during the generation of 'spindle' waves in which 1–2 s duration epochs of rhythmic, high frequency (250–500 Hz) bursts of action potentials are generated at an interburst frequency of between 7 and 14 Hz (see Steriade & Deschênes, 1984). Similarly, activation of corticothalamic afferents during periods of drowsiness, anaesthesia, or slow-wave sleep also result in the appearance of rhythmic burst firing in NRT neurones in the frequency range of spindle oscillations (e.g. Mulle *et al.* 1986). Intracellular recordings *in vivo* indicate that this activity is generated through the interaction of the arrival of barrages of excitatory postsynaptic potentials, presumably from bursting relay neurones and the low threshold Ca^{2+} spike of NRT cells (Mulle *et al.* 1986; Shosaku *et al.* 1989). Although the relative importance of synaptic and intrinsic properties of NRT cells to the generation of spindle oscillations are not yet clear, isolation of the NRT from all cortical and thalamic inputs has been reported to leave a nucleus in which the ability to generate spindle-like oscillations, either spontaneously or in response to electrical stimulation of the cut corticothalamic fibres, remains intact (Steriade, Domich & Oakson, 1987*a*). This result implies that the NRT contains within it the neural mechanisms required to generate rhythmic spindle-like oscillations. Indeed, intracellular recordings in guinea-pig NRT neurones maintained *in vitro* have revealed these cells to have the intrinsic ability to generate rhythmic low threshold Ca^{2+}-spike mediated bursts of action potentials (Avanzini, de Curtis, Panzica & Spreafico, 1989; McCormick & Wang, 1991), an oscillatory activity which has been proposed to arise from the interaction of the low threshold Ca^{2+} current and a Ca^{2+}-activated K^+ current (Avanzini *et al.* 1989).

The transition from slow-wave sleep to the waking state is associated with an abolition of rhythmic burst firing and the appearance of tonic, single spike activity in NRT neurones (Steriade *et al.* 1986). In behaving animals, this tonic activity often occurs as periods of highly regular discharge in the frequency range of 30–60 Hz (Mukhametov *et al.* 1970*b*; Marczynski, Burns, Livezey, Vimal & Chen, 1984). Recently, Pinault & Deschênes (1992*a*, *b*) have proposed that this activity arises from an interaction of the intrinsic membrane properties of NRT cells and the actions of modulatory neurotransmitters, particularly noradrenaline and acetylcholine, which are known to have potent excitatory and inhibitory effects, respectively, on these cells (McCormick & Prince, 1986; McCormick & Wang, 1991).

In the present report we investigate the ionic mechanisms by which NRT neurones generate rhythmic burst firing in the frequency range of spindle waves and tonic, single spike activity in the 30–80 Hz range.

METHODS

Methods for preparation of thalamic slices and recording from NRT neurones are similar to those published previously (McCormick & Wang, 1991). Male or female adult, Hartley guinea-pigs were deeply anaesthetized with sodium pentobarbitone (35 mg/kg I.P.) and killed by decapitation. The region of brain containing the reticular thalamic nucleus was removed, placed in cold (5 °C) bathing solution, and sectioned as 400 μm thick slices on a Vibratome (Pelco, Irvine, CA, USA). Thalamic slices were placed in an interface-style recording chamber (Fine Science Tools, Foster City, CA, USA) and allowed to recover for at least 2 h before recording commenced. The bathing medium contained (mM): NaCl, 124; KCl, 2·5; $MgSO_4$, 1·2; $NaPO_4$, 1·25; $CaCl_2$, 2; $NaHCO_3$, 26; dextrose, 10 and was aerated with 95 % O_2–5 % CO_2 to a final pH of 7·4. Recordings were made with the slices typically at the temperature of 35·5 °C, unless otherwise indicated.

Agonists were dissolved in the bathing medium and were applied with the pressure-pulse technique in which a brief pulse of pressure (10–100 ms; 200–350 kPa) to a broken micropipette (tip diameter 2–10 μm) was used to extrude volumes of 2–20 pl. Antagonists were typically applied through addition to the bathing medium. Extracellular single unit recordings were obtained with tungsten microelectrodes (Frederick Haer Corporation, Brunswick, ME, USA), while intracellular recordings were obtained with microelectrodes formed on a Sutter Instruments (Novato, CA, USA) P-80/PC micropipette puller, filled with 4 M potassium acetate, and bevelled to a final resistance of 70–100 MΩ. Bevelled electrodes with a relatively high resistance were found to be necessary to obtain high quality intracellular recordings from NRT cells without substantial damage to the neurone.

The NRT of the guinea-pig was readily visible in the dissecting microscope or to the unaided eye during the course of the experiments. Immunohistochemical staining for the GABA synthetic enzyme glutamic acid decarboxylase has previously been performed to confirm our localization of this nucleus in this recording situation (McCormick & Prince, 1986).

Extracellular single unit recordings were displayed on a chart recorder (Gould Instruments, Cleveland, OH, USA) by conversion of the data to an average spike frequency histogram through a comparator, counter and digital-to-analog converter (e.g. Fig. 10). Each occurrence of an action potential is reflected as a step increment in pen position on the chart recorder. After a pre-set time period (typically 2 s) the counter was reset. Therefore the height of each bin is representative of the average firing rate during that time period.

RESULTS

Intracellular recordings were obtained from ninety-three neurones and extracellular recordings from twenty-nine neurones in the guinea-pig nucleus reticularis thalami. Extracellular recordings from neurones in the guinea pig NRT revealed that these cells typically are either silent or discharging in a tonic, single spike manner. Electrical stimulation of the axons lateral to the NRT, which contains the corticothalamic tract, resulted in a burst of action potentials in NRT cells followed by a cessation of activity for about 1 s. This silent period could be followed by a sequence of 1–10 high frequency (250–400 Hz) burst discharges, which occurred at a rate of 3–7 Hz at 35 °C (Fig. 1*A*). Intracellular recordings of this activity revealed that it was associated with a fast EPSP-mediated burst of action potentials, as reported previously (Mulle *et al.* 1986; de Curtis, Spreafico & Avanzini, 1989), followed by a hyperpolarization and a subsequent rhythmic sequence of low threshold Ca^{2+}-spike mediated bursts and after-hyperpolarizations (Fig. 1*B*). Hyperpolarization of the neurone blocked the oscillatory activity and did not reveal any underlying synaptic events which may generate this activity (except for the initial EPSP), suggesting that it may be an intrinsic oscillation (not shown).

Intracellular injection of hyperpolarizing and depolarizing current pulses into NRT cells revealed the generation of action potentials in two distinct modes: rebound rhythmic burst firing and tonic, single spike activity (Fig. 2). As with synaptic activation, rebound rhythmic burst firing was associated with the

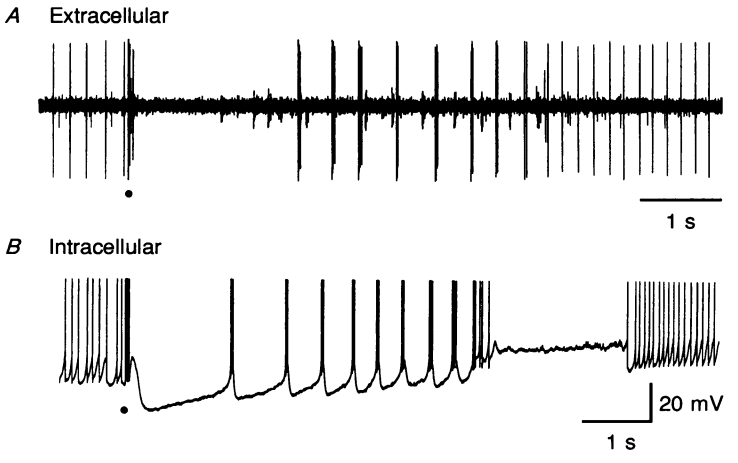

Fig. 1. Rhythmic response of nucleus reticularis cells to orthodromic activation. *A*, electrical stimulation of afferents lateral to the NRT results in a burst of action potentials followed by an inhibitory pause, followed by rhythmic burst firing in a guinea-pig NRT cell recorded extracellularly. *B*, intracellular recording of this activity revealed that the burst of action potentials is associated with a large excitatory postsynaptic potential followed by a hyperpolarization of the membrane potential and the rhythmic appearance of low threshold Ca^{2+} spike-mediated bursts of action potentials and burst after-hyperpolarizations (spike threshold is −55 mV).

rhythmic occurrence of low threshold Ca^{2+} spikes and after-hyperpolarizations (Fig. 2*A*), with the number of action potentials occurring during each high frequency burst discharge gradually decreasing and giving way to a tonic 'tail' of single spike activity (Fig. 2*A*). Depolarization of NRT cells from resting membrane potential resulted in the occurrence of single spike activity with a threshold firing rate of around 10 Hz, with little evidence of spike frequency adaptation (Fig. 2*C*). In contrast to relay neurones in the lateral geniculate nuclei, the transition between rhythmic burst firing and single spike activity could occur with depolarization of the membrane potential of only a few millivolts, a finding which may result from the depolarized level of T-current (transient-current) activation in these cells (Huguenard & Prince, 1992). This is well illustrated with the injection of triangular current pulses (Fig. 2*E*). Here, during the rising phase of the current pulse, NRT cells generate first a rhythmic sequence of burst discharges followed by single spike activity, which is then itself followed by the transition to single spike activity only after an additional few millivolts of depolarization (Fig. 2*E*).

Changes in the baseline membrane potential of NRT cells through the intracellular injection of current resulted in repeatable and typical changes in the

pattern of activity generated following the offset of a hyperpolarizing current pulse. For example, in the cell illustrated in Fig. 3*A*, injection of a hyperpolarizing current pulse at −70 mV results in two rebound burst discharges with an interburst frequency of 2·4 Hz. Depolarization of the neurone to −67 and −64 mV results in a

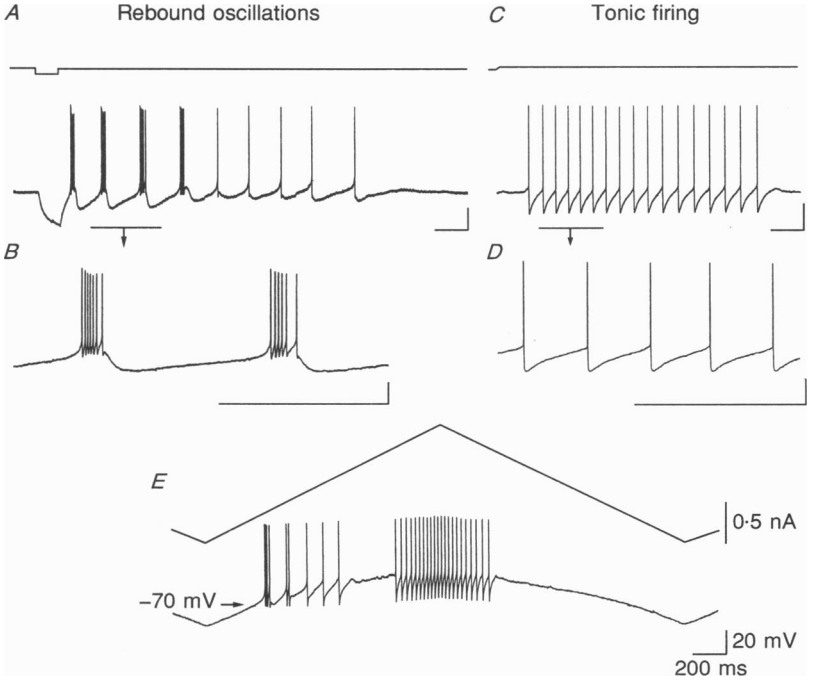

Fig. 2. Rebound oscillatory and tonic firing properties of NRT cells. *A*, injection of a hyperpolarizing current pulse at −68 mV results in a rebound period of rhythmic burst firing followed by tonic, single spike activity. *B*, expansion of two of the rhythmic bursts in *A* for detail. *C*, depolarization of a NRT cell results in highly regular single spike activity at 12 Hz. *D*, expanded portions of *C* shown for detail. *E*, intracellular injection of a triangular current pulse illustrates the voltage dependence of the different firing modes of NRT cells. All time scale bars are 200 ms and voltage scale bars are 20 mV. *A–D* are from the same neurone.

substantial increase in both the number of bursts generated and the interburst frequency. Additional depolarization to −61 mV increased the interburst frequency to approximately 11–15 Hz and enhanced the occurrence of a prolonged tail of single spike activity following rhythmic burst firing (Fig. 3*A*, −61 mV). Interestingly, as the tonic tail of single spike activity failed, a depolarizing potential occurred in the temporally correct position for the generation of the next action potential (Fig. 3*A*, −61 and −64 mV). Although the ionic basis of this depolarizing potential has not been investigated, we suggest that it may have a significant contribution from the low threshold Ca^{2+} current and result from the de-inactivation of a portion of this current by the single spike after-hyperpolarization (AHP). This finding indicates that the low threshold Ca^{2+} current may contribute significantly to single spike activity, although this hypothesis remains to be tested.

The intrinsic nature of the oscillatory burst firing is indicated by the lack of rhythmic synaptic potentials upon hyperpolarization, the sensitivity of the frequency of oscillation on the membrane potential of the cell (Fig. 3*A*), and the effects of block of voltage-dependent Na^+ channels with tetrodotoxin (Fig. 3*B* and

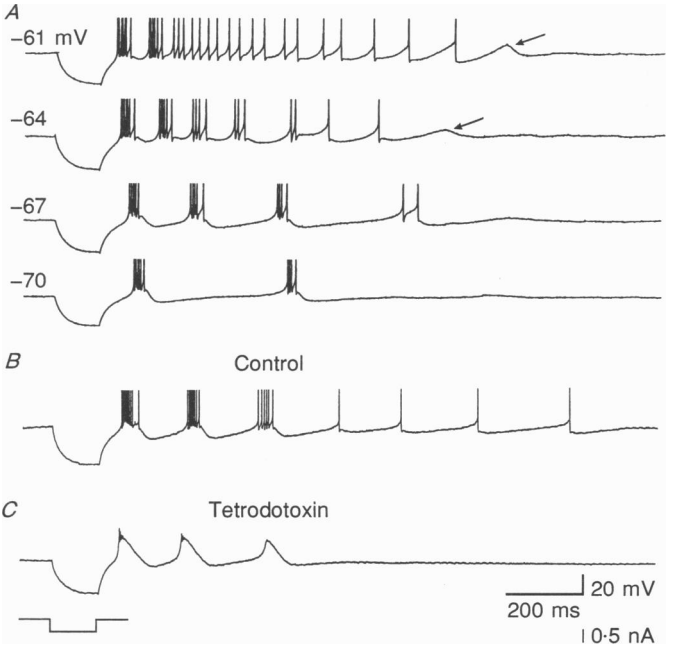

Fig. 3. Voltage dependence of rhythmic burst firing followed by tonic activity. *A*, injection of a hyperpolarizing current pulse into a guinea-pig NRT cell at −61 mV results in a rebound sequence of rhythmic bursts at approximately 11–15 Hz followed by a tonic tail of single spike activity. Note the subthreshold depolarizing potential which follows this tonic activity (arrow). Hyperpolarization of the cell to −64 mV reduces the tonic tail of activity and reveals rhythmic burst firing at 7–11 Hz. Hyperpolarization of the cell to −67 and −70 mV further reduces the sequence of activity and slows the frequency of rhythmic burst firing. *B*, intracellular injection of a hyperpolarizing current pulse results in a rebound oscillatory burst sequence followed by short period of single spike activity. *C*, local application of tetrodotoxin (10 μM in micropipette) results in an abolition of the fast spikes and reveals the underlying sequence of low threshold Ca^{2+} spikes. *A* and *B–C* are recorded from two different cells.

C). Local application of tetrodotoxin (10 μM in micropipette) resulted in the abolition of Na^+ action potentials and revealed the underlying low threshold Ca^{2+} spikes (Fig. 3*B* and *C*). These Ca^{2+} spikes were often associated with a preservation of the after-hyperpolarization which occurs in between each Ca^{2+} spike (Fig. 3 *C*; $n = 10$), although in some neurones this after-hyperpolarization was reduced by application of tetrodotoxin ($n = 7$). The latter finding indicates that the Na^+-dependent action potentials contribute to the after-hyperpolarization either

through the additional entry of Ca^{2+} into the cell (such as through high threshold Ca^{2+} channels), or through the release of inhibitory neurotransmitters, such as GABA, which may then also contribute to the AHP.

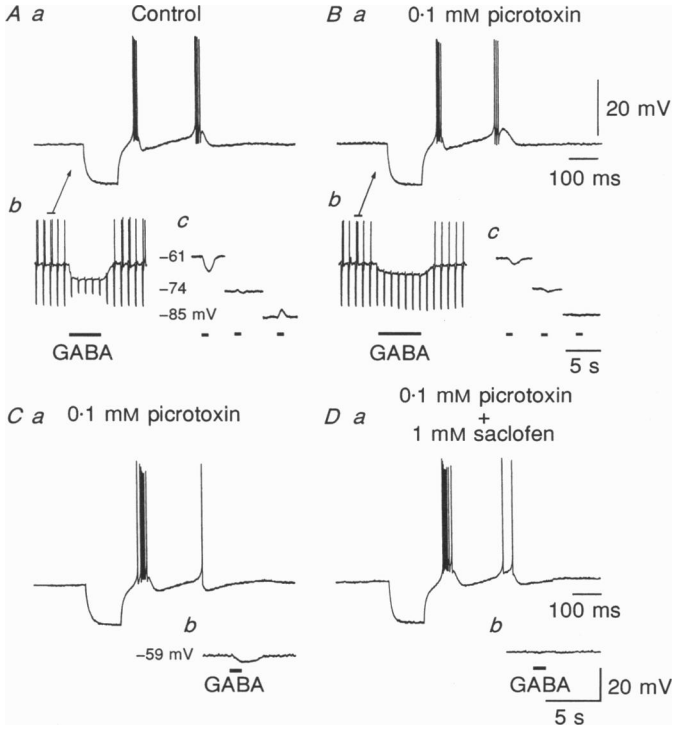

Fig. 4. Lack of effect of block of $GABA_A$- or $GABA_B$-mediated responses on rebound, rhythmic burst firing in NRT cells. *A a*, injection of a hyperpolarizing current pulse at −64 mV results in a rhythmic sequence of two burst discharges. Prolonged (*A b*) or brief (*A c*) application of GABA results in a hyperpolarizing response and an increase in membrane conductance, which reverses around −74 mV. *B*, bath application of picrotoxin (100 μM) does not affect rebound rhythmic burst firing (*B a*), and transforms the GABA response to one typical for activation of $GABA_B$ receptors, in which the reversal potential is around −85 mV in this cell. *C*, injection of a hyperpolarizing current pulse at −65 mV results in a rhythmic sequence of burst firing in a cell obtained in 100 μM picrotoxin while application of GABA results in a hyperpolarization. Local application of the $GABA_B$ antagonist 2-hydroxy-saclofen blocks the response to GABA, but does not affect rhythmic burst firing in this cell. Same cells before and after antagonist application.

To test the possible involvement of activation of GABAergic receptors in the generation of rhythmic burst firing, we applied the $GABA_A$ antagonist picrotoxin (100 μM in bath) and the $GABA_B$ antagonist 2-hydroxy-saclofen (1 mM in micropipette) to NRT cells. The effectiveness of these antagonists in blocking $GABA_A$ and $GABA_B$ receptors was examined by testing the effects of application of GABA on the recorded cell. In normal cells application of GABA resulted in a hyperpolarization and a marked increase in membrane conductance (Fig. 4*A b*). Eliciting this response at different membrane potentials revealed a reversal potential of around −74 mV (Fig. 4*A c*; $n = 3$). Bath application of picrotoxin

resulted in a shift in the GABA response reversal potential to −85 mV (Fig. 4*Bc*) and a marked reduction of the increase in membrane conductance (Fig. 4*Bb*), and had no effect on the rhythmic burst of action potentials generated in this cell (cf.

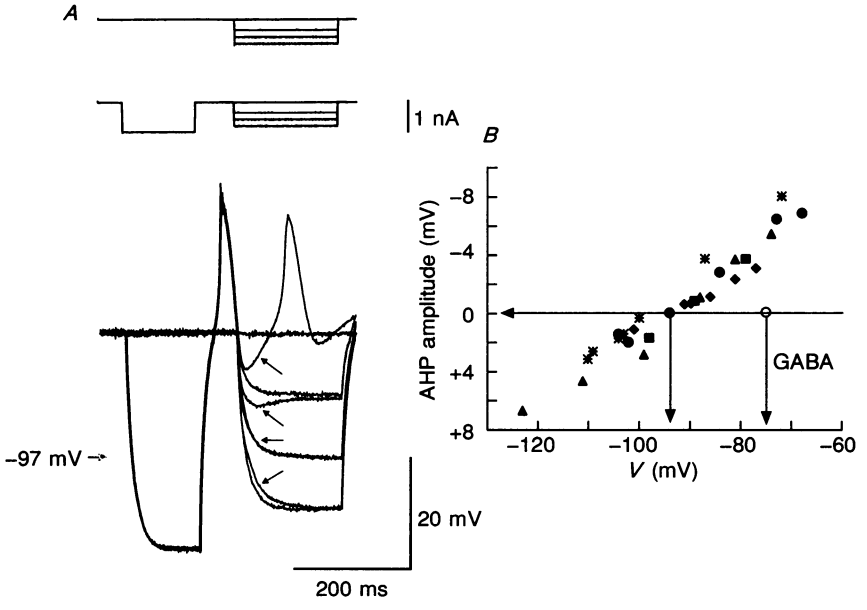

Fig. 5. Reversal potential of the burst after-hyperpolarization. *A*, injection of a hyperpolarizing current pulse results in a rhythmic sequence of two low threshold Ca^{2+} spikes separated by an after-hyperpolarization. The reversal potential of the after-hyperpolarization was examined by injecting a hyperpolarizing current pulse at the peak of the after-hyperpolarization and comparing the resulting deviation in membrane potential with that obtained by injection of the same current pulse during the lack of an after-hyperpolarization. In this cell, the AHP (arrows) reversed from hyperpolarizing (top two traces) to depolarizing (bottom traces) at about −97 mV (third set of traces from top). *B*, plot of the group data reveals an average reversal potential of -94 mV. The reversal potential for short latency responses to GABA (−75 mV) is shown for comparison.

Fig. 4*Aa* and *Ba*). Similarly, cells obtained in the presence of picrotoxin responded with normal sequences of rhythmic burst firing to the injection of a hyperpolarizing current pulse (Fig. 4*Ca*; $n = 7$). Local application of the $GABA_B$ antagonist 2-hydroxy-saclofen blocked the residual response of these cells to GABA (Fig. 5*Cb* and *Db*; $n = 2$) but did not disrupt the rhythmic burst firing (cf. Fig. 4*Ca* and *Da*). These results indicate that activation of $GABA_A$ and $GABA_B$ receptors do not contribute critically to the rhythmic burst firing recorded in the present experimental situation.

Ionic basis of burst after-hyperpolarization

Previous investigations of after-burst hyperpolarizations in thalamic neurones have revealed that there are at least two prominent mechanisms for their generation: activation of a Ca^{2+}-activated K^+ current (McCormick & Prince, 1988) or deactivation and activation of a hyperpolarization-activated cation current

(McCormick & Pape, 1990). If the burst AHP is a Ca^{2+}-activated K^+ current, then it should reverse to a depolarization at E_K, should be associated with a conductance increase, and should be blocked by blockers of K^+ currents (e.g. internal Cs^+, external tetraethylammonium or apamin) (see Rudy, 1988; Castle, Haylett & Jenkinson, 1989).

Intracellular injection of a short duration (10–20 ms) hyperpolarizing current pulse at the peak of the AHP revealed that this after-hyperpolarization is associated with an increase in apparent membrane conductance, suggesting that it is mediated by the opening of some type of ionic channels (not shown). Examination of the reversal potential of the low threshold Ca^{2+} spike AHP revealed that it reversed to an after-depolarization at an average membrane potential of −95 mV (± 2; $n = 5$; Fig. 5), which is close to the equilibrium potential for K^+ in 2·5 mM $[K^+]_o$ (McCormick & Prince, 1986), suggesting that the increase in membrane conductance is largely specific for K^+ ions. The occurrence of this K^+ conductance following a low threshold Ca^{2+} spike suggests that it may be Ca^{2+} activated. Indeed, increasing the buffering of $[Ca^{2+}]_i$ by including the Ca^{2+} chelating agent ethyleneglycol-bis-(β-aminoethyl ether)*N,N,N',N'*-tetraacetic acid (EGTA) in the recording micropipette resulted in the disappearance of the burst AHP and the appearance of a pronounced slow after-depolarization (Fig. 6*A*; $n = 20$). Block of fast action potentials with tetrodotoxin revealed a large slow after-depolarization underlying this event (not shown).

Further evidence that a Ca^{2+}-activated K^+ current underlies the generation of the burst-AHP was obtained by examining the effects of intracellular injection of the K^+ channel blocking agent Cs^+, bath application of either tetraethylammonium (TEA) or the bee venom toxin apamin. Intracellular recording of NRT neurones with caesium acetate microelectrodes resulted in the disappearance of after-burst hyperpolarizations and their replacement with a prolonged after-depolarization (Fig. 6*B*; $n = 4$; within-cell comparison). Application of tetrodotoxin (10 μM) blocked Na^+-dependent action potential generation but not the slow after-depolarization, indicating that this event is intrinsic to NRT cells (Fig. 6*B*).

Similarly, bath application of TEA (5–20 mM; $n = 3$) after the block of action potentials with tetrodotoxin also resulted in the slowing of the falling phase of the low threshold Ca^{2+} spike, a reduction in the membrane potential reached by the after-hyperpolarization, and the appearance of a large slow after-depolarization in single cells (Fig. 6*C*). However, even in the presence of 10 mM TEA, each low threshold Ca^{2+} spike was associated with a small after-hyperpolarization (Fig. 6*C*, TEA). Removal of TEA from the bathing medium reinstated the normal low threshold Ca^{2+} spike and after-hyperpolarization (Fig. 6*C*, wash).

Apamin is reported to block potently a particular subtype of Ca^{2+}-activated K^+ current and the underlying channels (reviewed in Castle *et al.* 1989). Local application of apamin (100 nM in micropipette; $n = 19$) resulted in a complete abolition of the Ca^{2+} spike after-hyperpolarization and resulted in the appearance of a prolonged after-depolarization (Fig. 6*D*). These effects of apamin were practically irreversible and prolonged (hours) washing with normal solution failed to reinstate the after-hyperpolarization, as reported previously (Avanzini *et al.* 1989).

These results indicate that the after-hyperpolarization occurring following the

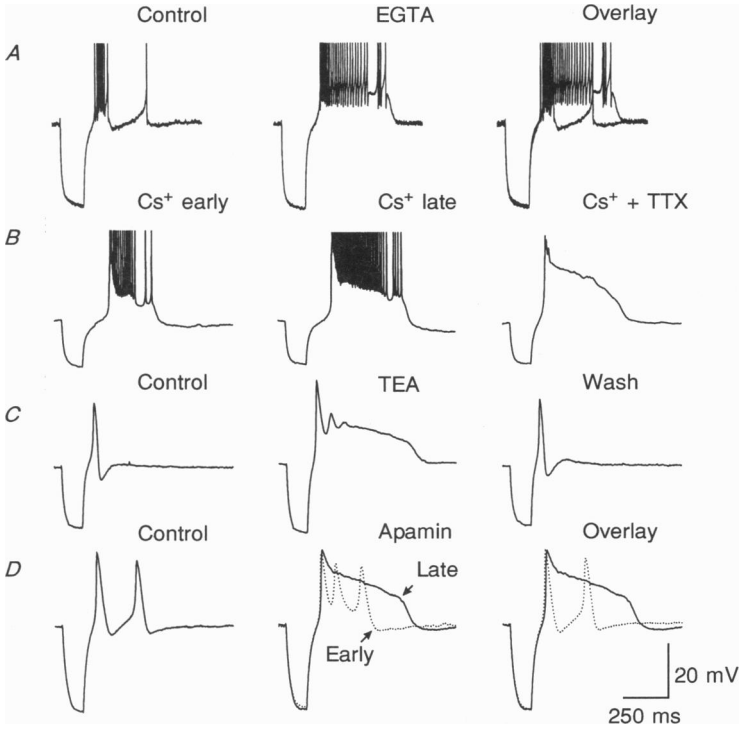

Fig. 6. Pharmacological properties of the burst after-hyperpolarization. *A*, buffering of intracellular Ca^{2+} blocks the burst after-hyperpolarization. Recording of cells with microelectrodes which contain a high concentration of EGTA (0·4 M EGTA + 1 M potassium acetate) results in an abolition of the burst after-hyperpolarization, a dramatic increase in action potential discharge rate during the burst, and the appearance of a tonic tail of activity (pre-pulse membrane potential (V_m) = −63 mV). *B*, recording NRT neurones with microelectrodes filled with 4 M caesium acetate results in an abolition of the burst after-hyperpolarization and the appearance of a large and prolonged after-depolarization (V_m = −65 mV). Local application of TTX (10 μM) abolishes the action potentials and reveals the underlying slow after-depolarization. *C*, bath application of tetraethylammonium (TEA; 10 mM) results in the appearance of a large slow after-depolarization, and the reduction of the negative value of the membrane potential obtained after the low threshold Ca^{2+} spike, although a burst after-hyperpolarization is still evident. These effects are reversible upon removal of TEA (wash; V_m = −68 mV). *D*, local application of apamin (100 nM in micropipette) results in a complete block of the after-hyperpolarization and the appearance of the slow after-depolarization (V_m = −63 mV). Action potentials blocked in *C* and *D* with local application of tetrodotoxin. Cells in *A*, *B*, *C* and *D* are from different experiments.

generation of a Ca^{2+} spike represents a Ca^{2+}-activated K^+ current. The hyperpolarization-activated (h)-current (McCormick & Pape, 1990) does not appear to make a critical contribution in NRT cells, since complete block of this current with local or bath application of Cs^+ (2 mM in bath; 20 mM in micropipette; $n = 4$) did not alter or block rhythmic burst firing (not shown).

Ionic basis of the after-depolarization

The ionic mechanisms involved in the generation of the after-depolarization which occurs after block of Ca^{2+}-activated K^+ currents was investigated in neurones after the block of voltage-dependent Na^+ currents with local applications

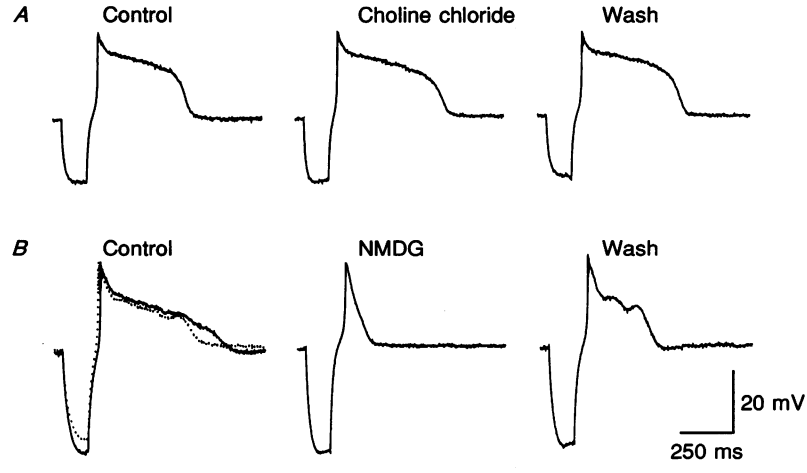

Fig. 7. Ionic basis of the slow after-depolarization. *A*, substitution of choline chloride for NaCl and choline bicarbonate for sodium bicarbonate in the bathing medium has little effect on the slow after-depolarization (prepulse $V_m = -63$ mV). *B*, in contrast, substitution of *N*-methyl-D-glucamine chloride for NaCl results in a selective block of the slow ADP ($V_m = -60$ mV). This effect is reversible. Two controls are shown in *B*. The continuous trace is a voltage pulse which matches that in NMDG, while the dotted line is one which matches that obtained during wash. Data obtained after application of tetrodotoxin (10 μM in micropipette) and apamin (100 nM in micropipette) to facilitate the study of the ADP. Data for *A* and *B* obtained from two seperate cells.

of tetrodotoxin (10 μM) and the Ca^{2+}-activated K^+ current with apamin (100 nM in micropipette). Under these circumstances, injection of hyperpolarizing current pulses were followed by a slow after-depolarization, as reported above (Figs 7 and 8). The possibility that this slow after-depolarization may be generated by a calcium-activated non-selective cation current (CAN-current; Partridge & Swandulla, 1988) was investigated with ion substitution experiments.

Substitution of choline chloride for NaCl and choline bicarbonate for sodium bicarbonate in equimolar concentrations in the bathing medium resulted in little effect on the slow after-depolarization (Fig. 7*A*; $n = 6$), while substituting *N*-methyl-D-glucamine chloride for NaCl resulted in an abolition of the slow ADP while leaving the low threshold Ca^{2+} spike intact (Fig. 7*B*; $n = 6$). Replacement of $CaCl_2$ in the bathing medium with $BaCl_2$ resulted in a marked enhancement of the low threshold Ca^{2+} spike, presumably owing to the block of K^+ currents and increased mobility of Ba^{2+} through T-channels (see Kostyuk, 1989), but did not block the slow ADP (Fig. 8*A*; $n = 3$). In contrast, replacement of $CaCl_2$ with $SrCl_2$ also resulted in an enhancement of the low threshold Ca^{2+} spike, but in association with a complete block of the slow ADP (Fig. 8*B*; $n = 4$).

In the experiment illustrated in Fig. 8*C*, $CaCl_2$ was replaced with $BaCl_2$, resulting in an enhancement of the low threshold Ca^{2+} spike and without block of the slow ADP. Replacement of $BaCl_2$ with $MgCl_2$ resulted initially in a reduction of the amplitude and rate of rise of the low threshold Ca^{2+} spike, and a complete block of the slow ADP. Further washing-in of the $MgCl_2$ resulted in a complete block of both

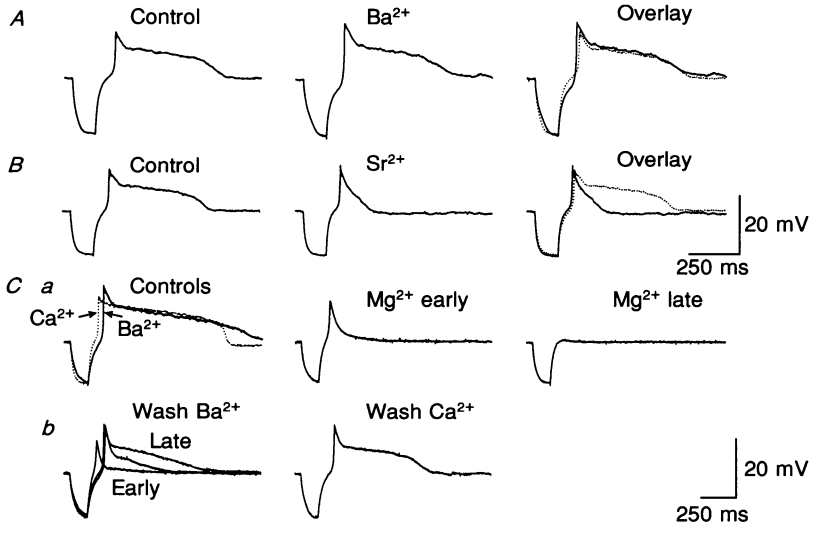

Fig. 8. Ionic mechanisms involved in activation of the slow ADP. *A*, replacement of $CaCl_2$ with $BaCl_2$ results in an increase in apparent input resistance (compensated for by reduction of the amplitude of the current pulse), an increase in the membrane time constant, an increase in the low threshold Ca^{2+} spike, and did not abolish the slow ADP (pre-pulse $V_m = -67$ mV). *B*, in contrast, replacement of $CaCl_2$ with $SrCl_2$ results in a complete abolition of the slow ADP and an enhancement of the low threshold Ca^{2+} spike ($V_m = -65$ mV). *Ca*, replacement of $CaCl_2$ with $BaCl_2$ again does not abolish the slow ADP, although replacement of $BaCl_2$ with $MgCl_2$ does abolish the slow ADP, followed by an abolition of the low threshold Ca^{2+} spike. These effects are reversible (*Cb*; $V_m = -72$ mV). Data obtained after application of tetrodotoxin (10 μM in micropipette) and apamin (100 nM in micropipette).

the low threshold Ca^{2+} spike and the slow ADP ($n = 3$). These effects of Mg^{2+} and Ba^{2+} were reversible (Fig. 8*Cb*).

Together these results suggest that the slow ADP is mediated by a Ca^{2+}-activated non-selective cation current which is able to be carried by both Na^+ and choline$^+$ but not by *N*-methyl-D-glucamine$^+$ and which can be activated by both Ca^{2+} and Ba^{2+} but not by Sr^{2+} or Mg^{2+}.

Ionic basis of tonic firing in NRT cells

Extracellular recordings of NRT cells revealed that application of 5-HT (500 μM in micropipette), noradrenaline (NA) (500 μM in micropipette) or 1S,3R-1-aminocyclopentane-1,3-dicarboxylic acid (ACPD; 500 μM in micropipette) resulted in marked excitation and the generation of tonic firing, as reported previously (McCormick & Wang, 1991). Interestingly, repeated application of any of these three substances resulted in a maximal firing frequency which, after being obtained,

could not be exceeded by additional application of the same agonist (e.g. Fig. 9*D*). This 'ceiling effect' was not due, however, to an inability of the cell to discharge tonically at higher frequencies, since additional applications of glutamate resulted in large increases in spike frequency (Fig. 9*D*). At 35 °C, the maximal frequency of firing which could be brought about by NA was 20–30 Hz ($n = 3$), while at 38 °C it

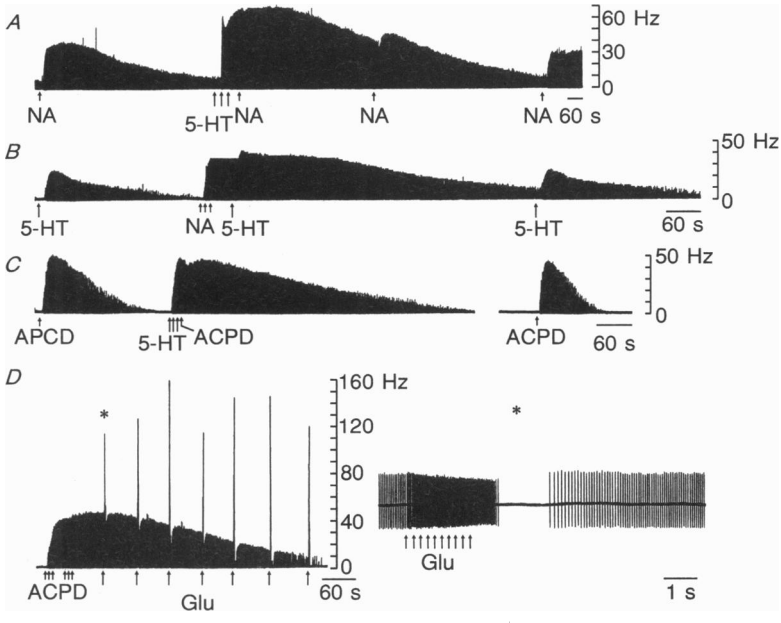

Fig. 9. Frequency limitation and non-additivity of tonic firing responses to NA, 5-HT and ACPD. *A*, application of NA (500 μM in micropipette) results in an increase in single spike discharge to approximately 40 Hz. Maximal application of 5-HT (500 μM in micropipette) results in a tonic discharge which becomes steady around 70 Hz. Application of NA at this point has no additional effect, indicating occlusion. As the response to 5-HT recovers, the response to NA reappears. *B*, in contrast, maximal application of NA, although reducing the response to 5-HT, does not completely occlude it. *C*, application of the glutamate metabotropic agonist ACPD (500 μM in micropipette) results in a peak increase in firing rate of approximately 50 Hz. Application of 5-HT and ACPD together result in a similar increase in firing rate. *D*, maximal application of ACPD results in a firing rate of approximately 50 Hz, which is not the maximal firing rate capable of being generated by the cell, since application of glutamate results in large increases in firing rate up to 160 Hz (original recording shown at right for detail). Guinea-pig NRT cell recorded at 38 °C.

was 35–40 Hz ($n = 3$). In contrast, both 5-HT ($n = 24$) and ACPD ($n = 11$) resulted in higher maximal firing frequencies of 40–70 Hz at 38 °C. The possibility that these agents may occlude one another owing to convergence of postsynaptic effector mechanisms was tested by examining the effects of maximal activation of one response on the others. Maximal activation of the serotonin response was found to block the response to NA and ACPD (Fig. 9*A* and *C*) while maximal activation of the NA response strongly reduced, but did not completely block the response to either 5-HT or ACPD (Fig. 9*B*). The possibility that a persistent Na^+ current may

contribute to the 5-HT-induced tonic depolarization was tested through the local application of tetrodotoxin (10 μM in micropipette). Local application of tetrodotoxin resulted in a cessation of action potential generation followed by a 5–6 mV hyperpolarization of the membrane potential (Fig. 10), presumably resulting from block of the persistent Na^+ current. Interestingly, during the

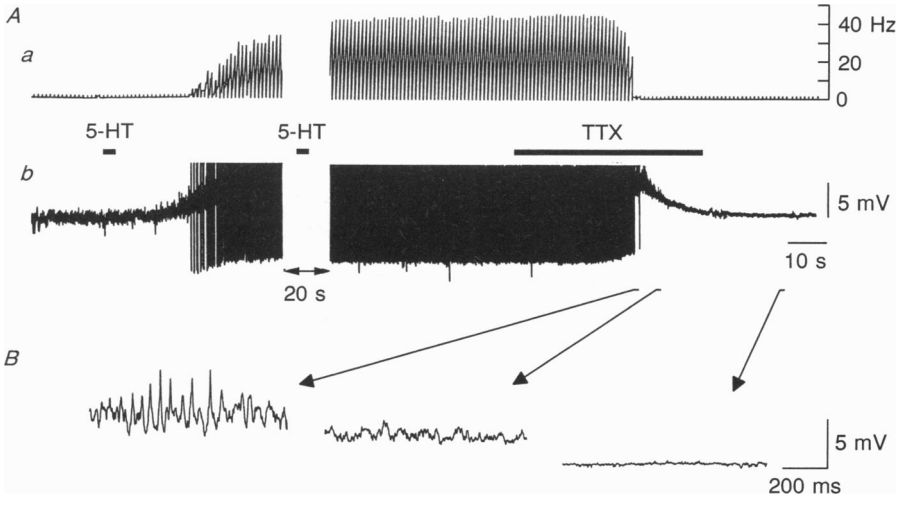

Fig. 10. Intracellular phenomena associated with the serotonin-induced tonic firing. *A a* and *A b*, application of a maximal does of 5-HT results in depolarization of the membrane potential (*A a*), an increase in membrane oscillation (not shown), and tonic firing which remains steady at approximately 45 Hz (*A b*; V_m prior to 5-HT = −58 mV). Block of voltage-dependent Na^+ channels with local application of tetrodotoxin (10 μM in micropipette) results in abolition of action potentials, followed by abolition of rhythmic oscillations (shown in *B* for detail) and hyperpolarization of the membrane potential.

application of tetrodotoxin, oscillations in the membrane potential were revealed (Fig. 10*B*). Similar oscillations in the membrane potential were also observed in normal cells during hyperpolarization below firing threshold (not shown). The eventual block of these oscillations by tetrodotoxin (Fig. 10*B*, right trace) indicates that they probably originate from a mixture of intrinisic membrane events and synaptic potentials, although this requires further investigation.

Application of the inhibitory amino acid GABA during tonic discharge induced by 5-HT or NA could reduce the firing frequency or inhibit all single spike activity (not shown). Cessation of the GABA application rapidly reinstated tonic discharge back to the original firing rate, while reinstatement of the GABA application again silenced neuronal activity (not shown). In this manner, application of GABA could 'sculpt' the firing rate of NRT cells with the maximal baseline firing rate being around 30–60 Hz.

Pinault & Deschênes (1992*a*) have recently suggested that NRT cells may have an intrinsic propensity to fire at 30–60 Hz. However, *in vitro*, NRT cells respond to 5-HT, NA, and ACPD with a steady increase in firing rate covering all frequencies between approximately 5 and 60 Hz (Fig. 9). To examine the possible tendency to

discharge at particular frequencies, we injected prolonged depolarizing current pulses (0·5–2 s) of varying amplitude into NRT cells and formed frequency *versus* current and frequency *versus* time plots (Fig. 11). Intracellular injection of constant current pulses into NRT cells were found to result in the generation of sustained

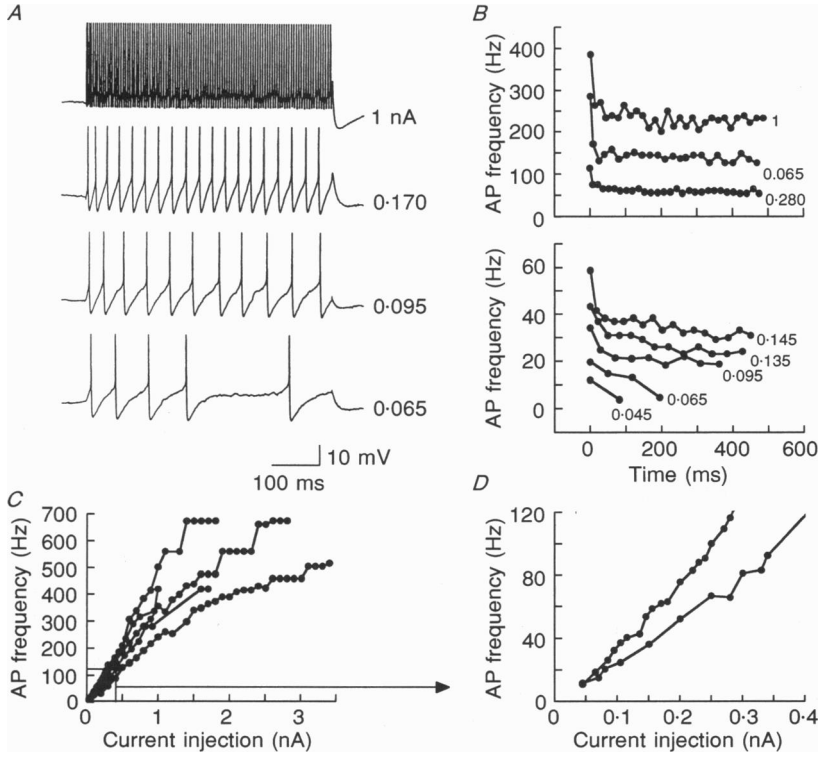

Fig. 11. Frequency *versus* current firing properties of NRT cells. *A*, examples of the response of a NRT cell to the intracellular injection of prolonged depolarizing current pulses of different magnitudes ($V_m = -56$ mV). *B*, frequency of firing *versus* time plots for frequency ranges of 0–400 and 0–70 Hz. Action potential discharge is associated with a slowing of firing in the first two interspike intervals followed by highly regular and maintained activity. *C*, plot of frequency *versus* current for the first interspike interval for five different cells reveal relatively linear relationships and the ability to fire at frequencies up to 500–700 Hz. *D*, detailed examination of the frequency *versus* current response curve at frequencies below 100 Hz for two cells reveals a threshold of approximately 10 Hz and no clear tendency to fire at any particular frequency.

trains of action potentials in which the frequency of firing slowed down over the first few interspike intervals to a steady state (Fig. 11*A* and *B*). Examination of the frequency *versus* current injected (*f–I*) plot for either the first interspike interval (Fig. 11*C* and *D*; $n = 8$) or for steady state (not shown) did not reveal any particular frequency between 10 and 400 Hz which was preferred by the NRT cells. Thus, small increases in the amount of injected current resulted in increases in firing rate in a linear manner, without the non-linearities predicted if these cells 'preferred' particular frequencies of activity (Fig. 11*D*).

DISCUSSION

The nucleus reticularis of the thalamus appears to be the 'pacemaker' of certain forms of slow oscillation in the thalamus, particularly spindle waves (reviewed in Steriade & Deschênes, 1984). Spindle waves are 1–3 s periods of 7–14 Hz oscillation which occur during light slow wave sleep with a marked periodicity of once every 5–10 s. Our results indicate that NRT neurones possess the ionic currents necessary to generate intrinsic rhythmic sequences or high frequency burst discharges in the frequency range of spindle waves (7–12 Hz) at body temperature. This sequence of oscillations appears to be mediated in large part through the activation of a low threshold Ca^{2+} spike, which generates a high frequency burst of Na^+- and K^+-dependent action potentials, followed by an after-hyperpolarization mediated by an apamin-sensitive Ca^{2+}-activated K^+ current (Fig. 12; see also Avanzini *et al.* 1989). This rhythmic burst firing may occur for two to eight cycles, presumably depending upon the amplitude of the Ca^{2+}-activated K^+ current and its interaction with the T-current (I_T). The intrinsic ability of NRT cells to generate rhythmic burst discharges may allow these cells to make a critical contribution to the generation of spindle waves in the thalamus. However, intracellular recordings from NRT cells *in vivo* during spontaneous spindle wave generation, or during rhythmic oscillation induced by single shock stimulation of cortical or thalamic inputs, reveal a significant contribution of excitatory synaptic potentials to the action potential discharge patterns of NRT cells (Mulle *et al.* 1986; Shosaku *et al.* 1989). Strong hyperpolarization of NRT cells during these events indicate that a barrage of EPSPs, presumably resulting from a burst of action potentials in one or more relay cells, results in the activation of additional depolarizing currents in NRT cells, such as I_T, and a subsequent burst discharge. We are then left with the question of whether spindle oscillations are generated as an intrinsic property of NRT cells or as synaptic events generated through their interaction with thalamic relay cells. Since surgical isolation of the NRT from the rest of the thalamus is reported to leave the NRT with the ability to generate spindle-like oscillations (Steriade *et al.* 1987*a*) and EPSPs of presumed thalamic origin occur in NRT cells during each cycle of the spindle wave, it would appear that both processes are involved. We propose the following scenario as one possible mechanism of spindle wave generation. The coincident burst firing of some critical number of NRT cells, either intrinsically or in response to cortical or thalamic input, results in the hyperpolarization of both these NRT cells (through a Ca^{2+}-activated K^+ current) and an anatomically connected population of relay cells (through GABAergic inhibition). As these periods of hyperpolarization lessen, the NRT cells, and a subset of relay cells, will generate an intrinsic burst of action potentials through the activation of I_T (see Andersen & Andersson, 1968; Steriade & Deschênes, 1984). Which cells will generate these bursts first will depend upon the kinetics and depth of the Ca^{2+}-activated K^+ current in the NRT cells and the inhibitory postsynaptic potential in the relay cells. If one or more of the relay cells which are inhibited bursts before the NRT cell, then the NRT cell will be depolarized by a barrage of one to five EPSPs arriving at 250–400 Hz depending on the number of spikes in the relay cell burst and the convergence of bursting relay cells to the NRT neurone.

This barrage of EPSPs will in turn activate the low threshold Ca^{2+} current in the NRT, the amount of which is available being determined by the duration and depth of after-hyperpolarization occurring after the last burst discharge. The activation of I_T will further enhance the depolarization resulting from the EPSPs, and result in a burst of action potentials in the NRT cells, which will begin the cycle again by hyperpolarizing the relay cells. Alternatively, the NRT cells may burst intrinsically before the arrival of thalamic EPSPs. In this circumstance the synaptic potentials will then facilitate the low threshold Ca^{2+} spike in the generation of action potentials and the occurrence of the two together will determine the depth and duration of the subsequent after-hyperpolarization in the NRT cell and the depth and duration of the inhibition of the connected relay cells. Together, both of these processes will subsequently determine the frequency and strength of oscillation.

If none of the relay cells contacting a particular NRT cell fire during one phase of the spindle wave, then the NRT cell may still generate a rebound burst of action potentials at approximately the correct interval, owing to the activation of the low threshold Ca^{2+} spike by the relaxation of the after-hyperpolarization. In this manner, the ability of NRT cells to generate rhythmic burst discharges allows for a 'safety mechanism' in which the rhythmic oscillation may continue even in the lack of rebound response from thalamic relay cells. Thus, we view the rhythmic firing of NRT cells during the generation of spindle waves as a mixture of intrinsic oscillatory properties and circuitous interactions between these cells and their anatomically connected relay cells. Both of these mechanisms of oscillation appear to have a similar resonant frequency (7–14 Hz), ensuring that even failure of the relay component of the oscillation will leave intact an oscillation in the NRT cell of a similar amplitude and time course.

Spindle waves in naturally sleeping cats, in contrast to those recorded in barbiturate-anaesthetized animals, are associated with the appearance of a prolonged tonic 'tail' of action potential activity in NRT cells after each sequence of rhythmic burst firing (Domich, Oakson & Steriade, 1986). In the present study we have shown that NRT cells are capable of generating a tonic tail of single spike activity after the generation of rhythmic low threshold Ca^{2+} spikes and that this tonic tail may be mediated by a slow after-depolarization, which itself may be generated through a Ca^{2+}-activated non-selective cation (CAN) current. Calcium-activated non-selective cation currents have been reported in some invertebrate neurones that are known to generate intrinsic and periodic bursts of action potentials (reviewed in Partridge & Swandulla, 1988). We propose that in NRT cells, the rhythmic occurrence of low threshold Ca^{2+} spikes and their associated bursts of fast action potentials results in increases in $[Ca^{2+}]_i$ which not only triggers a Ca^{2+}-activated K^+ current, but may also gradually activate I_{CAN}. As this cation current is activated, it depolarizes the cell towards single spike firing threshold and counteracts the hyperpolarizing influence of the Ca^{2+}-activated K^+ current. The loss of the postburst AHP results in a decrease in removal of inactivation of I_T, thereby resulting in an eventual failure of rebound low threshold Ca^{2+} spikes. Subsequently, the slow after-depolarization dominates the membrane potential and the cell discharges in a tonic manner.

Origin of tonic activity in NRT cells

Awakening from sleep is associated with an abolition of rhythmic burst firing in the NRT and the appearance of tonic, single spike activity, presumably through tonic depolarization of the membrane potential of NRT cells (e.g. Hirsch,

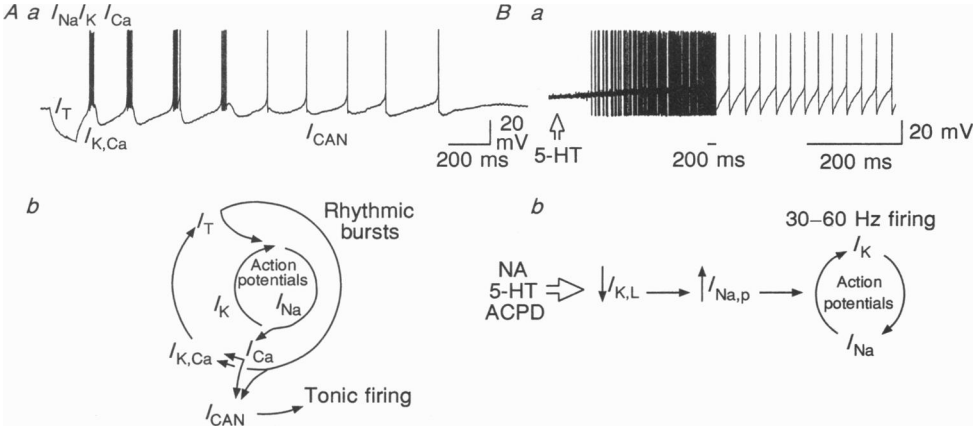

Fig. 12. Idealized scheme of the ionic basis of rhythmic burst and tonic firing in NRT cells. Removal of a hyperpolarizing current pulse results in a low threshold Ca^{2+} spike, which activates a high frequency burst of action potentials mediated by the transient Na^+ current I_{Na} and various K^+ currents, collectively referred to as I_K. In addition, the fast Na^+ spikes also are likely to activate high threshold Ca^{2+} currents, here referred to as I_{Ca}. The entry of Ca^{2+} results in the activation of Ca^{2+}-activated K^+ current ($I_{K,Ca}$) and therefore an after-hyperpolarization. The depth and duration of this after-hyperpolarization determines the amplitude of the subsequent low threshold Ca^{2+} spike, which is activated by the relaxation of the after-hyperpolarization. In addition to activating a Ca^{2+}-activated K^+ current, the entry of Ca^{2+} into the cell is also proposed to activate a Ca^{2+}-activated non-selective cation current (I_{CAN}) which results in a slow after-depolarization and the generation of tonic discharge at the end of the oscillatory burst firing (*A a* and *A b*). Activation of serotoninergic, noradrenergic or glutamate metabotropic receptors results in a tonic depolarization of the cell, in part through the reduction of a resting 'leak' potassium conductance $I_{K,L}$ which results in single spike activity in the frequency range of 30–60 Hz. The frequency of this tonic activity is proposed to be determined in large part by the interaction of the persistent Na^+ current ($I_{Na,p}$) and the currents involved in action potential generation (*Ba* and *Bb*).

Fourment & Marc, 1983; Steriade *et al.* 1986; see Steriade, Jones & Llinás, 1990). Of the numerous systems innervating the NRT, the cortical and thalamic inputs are known to exert an excitatory influence through excitatory amino acid receptors (de Curtis *et al.* 1989), the noradrenergic and serotoninergic inputs may tonically depolarize NRT cells through block of a K^+ current through activation of α_1 and 5-HT_2 receptors (Kayama, Negi, Sugitani & Iwama, 1982; McCormick & Wang, 1991), the cholinergic inputs may inhibit single spike activity through an increase in K^+ conductance through M_2 receptors (McCormick & Prince, 1986), and the

GABAergic inputs may inhibit neuronal activity through $GABA_A$ and $GABA_B$ receptors (Fig. 5). Therefore, the depolarization of NRT cells that is associated with the transition from the sleeping to the waking and attentive state would represent a balance of all of these influences (and probably others) and the intrinsic properties of NRT cells. Here we have shown that maximal activation of serotoninergic, noradrenergic, or glutamate metabotropic receptors on NRT cells in the absence of other transmitter actions results in the depolarization of these cells, increased activation of a persistent Na^+ current and the generation of 30–60 Hz tonic firing. This tonic firing may then be 'gated' on and off through the activation of GABAergic receptors. Similarly, Pinault & Deschênes (1992*a*,*b*) have recently described the presence of 'clock-like' firing of NRT neurones at frequencies between 25 and 60 Hz (centred around 40 Hz) in urethane anaesthetized rats. This activity is critically dependent upon noradrenergic influences, since lesions of the locus coeruleus or application of α_1 antagonists silences the tonically firing NRT cells. However, in addition, cooling of the cerebral cortex reduced the frequency of tonic activity while reduction of GABAergic transmission with the $GABA_A$ antagonist bicuculline or muscarinic transmission with scopolamine increases the rate of action potential discharge, indicating that this activity is under the influence of a number of convergent systems (Pinault & Deschênes, 1992*a*,*b*).

In summary, we suggest that NRT cells generate action potentials in three basic modes: at hyperpolarized membrane potentials, NRT cells may generate rhythmic bursts at relatively slow frequencies (e.g. 0·5–7 Hz; Fig. 3); at slightly more depolarized levels, NRT cells oscillate at higher frequencies (7–14 Hz) and generate rhythmic burst sequences followed by tonic single spike activity (Figs 3 and 12); while at still more depolarized levels, activity is dominated by the occurrence of highly regular, tonic activity (Fig. 12), the frequency of which is determined by the mixture of intrinsic ionic currents and convergence of neurotransmitter actions. The presence of these three different modes of action potential generation may allow NRT neurones to participate actively in the generation of the basic oscillatory rhythms seen in the forebrain: delta waves (0·5–4 Hz) during deep slow-wave sleep; spindle waves (7–14 Hz) during light slow-wave sleep; and gamma waves (30–60 Hz) during awake and attentive behaviour. Which of these different modes of activity is generated is determined through a co-ordinated modulation of thalamocortical systems by the ionic and cellular actions of the ascending and descending neurotransmitter systems, such that during periods of deep slow wave sleep the lack of activity in ascending noradrenergic, serotoninergic and cholinergic systems allows NRT, thalamic relay, and some cortical neurones to relax into the generation of slow (0·5–4 Hz) rhythmic burst firing (see also Steriade, Curró Dossi & Nunez, 1991), while small increases in activity in these ascending systems may depolarize NRT and thalamic relay cells into the 'spindle-oscillation' mode of light, synchronized electroencephalogram sleep. Further increases in activity in these ascending systems may induce a state of readiness in thalamocortical networks which includes the increased propensity for the transmission and processing of sensory information and the generation of 40 Hz oscillations (Steriade & McCarley, 1990 for review; McCormick, 1992). During these various changes in state of

activity in thalamocortical networks, we, and others (Crick, 1984; Steriade & Deschênes, 1984; Steriade & Llinás, 1988; Asanuma, 1989; Pinault & Deschênes, 1992*a*, *b*) envision the properties and connectivity of the NRT as ideal for the coordination of correlated activity in the forebrain; a hypothesis which requires detailed investigation.

Note added in proof. We have recently reported the occurrence of spindle waves in slices of Ferret LGNd and perigeniculate nucleus maintained *in vitro* (M. von Krosigt, T. Bal and D.A. McCormick, 1993. (Science, in the Press)). Perigeniculate neurons generate rhythmic bursts of low threshold Ca^{2+} spikes during these oscillations in similarity with those reported here although they are often activated by excitatory postsynaptic potentials arriving from the LGNd.

We thank Marcus von Krosigk and Zhong Wang for valuable comments on this manuscript. This research was supported by the National Institute of Health, the Klingenstein Fund and the Sloan Foundation.

REFERENCES

ANDERSEN, P. & ANDERSSON, S. A. (1968). *Physiological Basis of the Alpha Rhythm.* Appleton-Century-Crofts, New York.

ASANUMA, C. (1989). Axonal arborizations of a magnocellular basal nucleus input and their relation to the neurons in the thalamic reticular nucleus of rats. *Proceedings of the National Academy of Sciences of the USA* **86**, 4746–4750.

ASANUMA, C. (1992). Noradrenergic innervation of the thalamic reticular nucleus: A light and electron microscopic immunohistochemical study in rats. *Journal of Comparative Neurology* **319**, 299–311.

ASANUMA, C. & PORTER, L.L. (1990) Light and electron microscopic evidence for a GABAergic projection from the caudal basal forebrain to the thalamic reticular nucleus in rats. *Journal of Comparative Neurology* **302**, 159–172.

AVANZINI, G., DE CURTIS, M., PANZICA, F. & SPREAFICO, R. (1989). Intrinsic properties of nucleus reticularis thalami neurones of the rat studied *in vitro*. *Journal of Physiology* **416**, 111–122.

BUZSÁKI, G., BICKFORD, R. G., PONOMAREFF, G., THAL, L. J., MANDEL, R. & GAGE, F. H. (1988). Nucleus basalis and thalamic control of neocortical activity in the freely moving rat. *Journal of Neuroscience* **8**, 4007–4026.

CASTLE, N. A., HAYLETT, D. G. & JENKINSON, D. H. (1989). Toxins in the characterization of potassium channels. *Trends in Neurosciences* **12**, 59–65.

CRICK, F. (1984). Function of the thalamic reticular complex: The searchlight hypothesis. *Proceedings of the National Academy of Sciences of the USA* **81**, 4586–4590.

DE CURTIS, M., SPREAFICO, R. & AVANZINI, G. (1989). Excitatory amino acids mediate responses elicited *in vitro* by stimulation of cortical afferents to reticularis thalami neurons of the rat. *Neuroscience* **33**, 275–283.

DESCHÊNES, M., MADARIAGA-DOMICH, A. & STERIADE, M. (1985). Dendrodendritic synapses in cat reticularis thalami nucleus: a structural basis for thalamic spindle synchronization. *Brain Research* **334**, 169–171.

DOMICH, L., OAKSON, G. & STERIADE, M. (1986). Thalamic burst patterns in the naturally sleeping cat: A comparison between cortically projecting and reticularis neurones. *Journal of Physiology* **379**, 429–449.

HALLANGER, A. E., LEVEY, A. I., LEE, H. J., RYE, D. B. & WAINER, B. H. (1987). The origins of cholinergic and other subcortical afferents to the thalamus in the rat. *Journal of Comparative Neurology* **262**, 105–124.

HARRIS, R. M. (1987). Axon collaterals in the thalamic reticular nucleus from thalamocortical neurons in the rat ventrobasal thalamus. *Journal of Comparative Neurology* **258**, 397–406.

HAZRATI, L.-N. & PARENT, A. (1991). Projection from the external pallidum to the reticular thalamic nucleus in the squirrel monkey. *Brain Research* **550**, 142–146.

HIRSCH, J. C., FOURMENT, A. & MARC, M. E. (1983). Sleep-related variations of membrane potential in the lateral geniculate body relay neurons of the cat. *Brain Research* **259**, 308–312.

HOUSER, C. R., VAUGHN, J. E., BARBER, R. P. & ROBERTS, E. (1980). GABA neurons are the major cell type of the nucleus reticularis thalami. *Brain Research* **200**, 341–354.

HUGUENARD, J. R. & PRINCE, D. A. (1992). A novel T-type current underlies prolonged Ca^{2+}-dependent burst firing in GABAergic neurons of the rat thalamic reticular nucleus. *Journal of Neuroscience* **12**, 3804–3817.

JONES, E. G. (1985). *The Thalamus.* Plenum Press, New York.

KAYAMA, Y., NEGI, T., SUGITANI, M. & IWAMA, K. (1982). Effects of locus coeruleus stimulation on neuronal activities of dorsal lateral geniculate nucleus and perigeniculate reticular nucleus of the rat. *Neuroscience* **7**, 655–666.

KOSTYUK, P. G. (1989). Diversity of calcium ion channels in cellular membranes. *Neuroscience* **28**, 253–261.

LAVOIE, B. & PARENT, A. (1991). Serotoninergic innervation of the thalamus in primate: An immunohistochemical study. *Journal of Comparative Neurology* **312**, 1–18.

LEVEY, A. I., HALLANGER, A. E. & WAINER, B. H. (1987*a*). Cholinergic nucleus basalis neurons may influence the cortex via the thalamus. *Neuroscience Letters* **10**, 7–13.

McCORMICK, D. A. (1992). Neurotransmitter actions in the thalamus and cerebral cortex and their role in neuromodulation of thalamocortical activity. *Progress in Neurobiology* **39**, 337–388

McCORMICK, D. A. & PAPE, H.-C. (1990). Properties of a hyperpolarization-activated cation current and its role in rhythmic oscillation in thalamic relay neurons. *Journal of Physiology* **431**, 291–318.

McCORMICK, D. A. & PRINCE, D. A. (1986). Acetylcholine induces burst firing in thalamic reticular neurones by activating a potassium conductance. *Nature* **319**, 402–405.

McCORMICK, D. A. & PRINCE, D. A. (1988). Noradrenergic modulation of firing pattern in guinea pig and cat thalamic neurons, *in vitro*. *Journal of Neurophysiology* **59**, 978–996.

McCORMICK, D. A. & WANG, Z. (1991). Serotonin and noradrenaline excite GABAergic neurones of the guinea-pig and cat nucleus reticularis thalami. *Journal of Physiology* **442**, 235–255.

MARCZYNSKI, T. J., BURNS, L. L., LIVEZEY, G. T., VIMAL, R. L. P. & CHEN, E. (1984). Sleep and purposive behavior: Inverse deviations from randomness of neuronal firing patterns in the feline thalamus. A new form of homeostasis? *Brain Research* **298**, 75–90.

MUKHAMETOV, L. M., RIZZOLATTI, G. & SEITUN, A. (1970). An analysis of the spontaneous activity of lateral geniculate neurons and of optic tract fibers in freely moving cats. *Archives Italiennes de Biologie* **108**, 325–347.

MUKHAMETOV, L. M., RIZZOLATTI, G. & TRADARDI, V. (1970). Spontaneous activity of neurones of nucleus reticularis thalami in freely moving cats. *Journal of Physiology* **210**, 651–667.

MULLE, C., MADARIAGA, A. & DESCHÊNES, M. (1986). Morphology and electrophysiological properties of reticularis thalami neurons in cat: *in vivo* study of a thalamic pacemaker. *Journal of Neuroscience* **6**, 2134–2145.

OHARA, P. T. & LIEBERMAN, A. R. (1981). Thalamic reticular nucleus: anatomical evidence that cortico-reticular axons establish monosynaptic contact with reticulo-geniculate projection cells. *Brain Research* **207**, 153–156.

OHARA, P. T. & LIEBERMAN, A. R. (1985). The thalamic reticular nucleus of the adult rat: experimental anatomical studies. *Journal of Neurocytology* **14**, 365–411.

PARÉ, D., HAZRATI, L.-N., PARENT, A. & STERIADE, M. (1990). Substantia nigra pars reticulata projects to the reticular thalamic nucleus of the cat: a morphological and electrophysiological study. *Brain Research* **535**, 139–146.

PARTRIDGE, L. D. & SWANDULLA, D. (1988). Calcium-activated non-specific cation channels. *Trends in Neurosciences* **11**, 69–72.

PINAULT, D. & DESCHÊNES, M. (1992*a*). Voltage dependent 40-Hz oscillations in rat reticular thalamic neurons *in vivo*. *Neuroscience* **51**, 245–258.

PINAULT, D. & DESCHÊNES, M. (1992*b*). Control of 40-Hz firing of reticular thalamic cells by neurotransmitters. *Neuroscience* **51**, 259–268.

RUDY, B. (1988). Diversity and ubiquity of K channels. *Neuroscience* **25**, 729–749.

SHOSAKU, A., KAYAMA, Y., SUMITOMO, I., SUGITANI, M. & IWAMA, K. (1989). Analysis of recurrent inhibitory circuit in rat thalamus: Neurophysiology of the thalamic reticular nucleus. *Progress in Neurobiology* **32**, 77–102.

STERIADE, M., CURRÓ DOSSI, R. & NUNEZ, A. (1991). Network modulation of a slow intrinsic oscillation of cat thalamocortical neurons implicated in sleep delta waves: cortical potentiation and brainstem suppression. *Journal of Neuroscience* **11**, 3200–3217.

STERIADE, M. & DESCHÊNES, M. (1984). The thalamus as a neuronal oscillator. *Brain Research Reviews* **8**, 1–63.

STERIADE, M., DOMICH, L. & OAKSON, G. (1986). Reticularis thalami neurons revisited: Activity changes during shifts in states of vigilance. *Journal of Neuroscience* **6**, 68–81.

STERIADE, M., DOMICH, L. & OAKSON, G. (1987*a*). The deafferented reticular thalamic nucleus generates spindle rhythmicity. *Journal of Neurophysiology* **57**, 260–273.

STERIADE, M., JONES, E. G. & LLINÁS, R. R. (1990). *Thalamic Oscillations and Signaling.* John Wiley and Sons, New York.

STERIADE, M. & LLINÁS, R. R. (1988). The functional states of the thalamus and the associated neuronal interplay. *Physiological Reviews* **68**, 649–742.

STERIADE, M. & MCCARLEY, R. W. (1990). *Brainstem Control of Wakefullness and Sleep.* Plenum Press, New York.

STERIADE, M., PARENT, A. & HADA, J. (1984). Thalamic projections of nucleus reticularis thalami of cat: a study using retrograde transport of horseradish peroxidase and double fluorescent tracers. *Journal of Comparative Neurology* **229**, 531–547.

STERIADE, M., PARENT, A., PARÉ, D. & SMITH, Y. (1987*b*). Cholinergic and non-cholinergic neurons of cat basal forebrain project to reticular and mediodorsal thalamic nuclei. *Brain Research* **408**, 373–376.

WILSON, J. R. & HENDRICKSON, A. E. (1988). Serotonergic axons in the monkey's lateral geniculate nucleus. *Visual Neuroscience* **1**, 125–133.

YEN, C. T., CONLEY, M., HENDRY, S. H. C. & JONES, E. G. (1985). The morphology of physiologically identified GABAergic neurons in the somatic sensory part of the thalamic reticular nucleus in the cat. *Journal of Neuroscience* **5**, 2254–2268.